

Enhanced VUV-assisted high harmonic generation

A Heinrich, W Kornelis, M P Anscombe, C P Hauri, P Schlup, J Biegert and U Keller

ETH Zurich, Physics Department, Institute of Quantum Electronics, 8093 Zurich, Switzerland

E-mail: biegert@phys.ethz.ch

Received 10 January 2006, in final form 30 May 2006

Published 22 June 2006

Online at stacks.iop.org/JPhysB/39/S275

Abstract

We have enhanced extreme ultraviolet (XUV) harmonics around 90 eV in He using a combination of vacuum ultraviolet harmonics, generated in a Xe capillary, and the strong infrared (IR) laser pulse. With no changes in the IR input energy or the configuration of the He target, the collinearly focused combination of the two fields changed the spectral properties and increased the yield of the XUV harmonics compared to those generated with the IR field alone.

(Some figures in this article are in colour only in the electronic version)

1. Introduction

High harmonic generation (HHG) [1–4] has become an important and widely used method for generating laser-like radiation from the vacuum ultraviolet down to the extreme ultraviolet wavelength regime, the water window around 3 nm [5] and with the highest photon energies reaching 1.3 keV [6]. The generated radiation forms a plateau of similar-intensity harmonics separated by twice the frequency of the driving field followed by a cut-off of rapidly decreasing intensity [7]. The underlying physics of IR-driven HHG can be explained in a semi-classical three-step model [8–10] where a bound electron in an atom is first tunnel ionized, then accelerated in the driving field and finally recombined to the ground state emitting a high-energy photon.

Almost since its discovery, there has been an extensive effort to improve the efficiency of HHG. Most of these studies have focused on improving the macroscopic phase matching of the generated radiation and it was demonstrated that better phase matching in a noble gas jet can be achieved with different focusing geometries and by varying the position of the gas jet relative to the laser focus [11–14]. In particular, conversion efficiencies of about 10^{-5} in the 30 nm [15] and 10^{-7} in the 13 nm [16, 17] region were obtained using high-power IR laser pulses and a loose focusing geometry. Improved phase matching in hollow-core fibres [18] and filaments [19] has been demonstrated, but it is ultimately limited by reabsorption [20, 21].

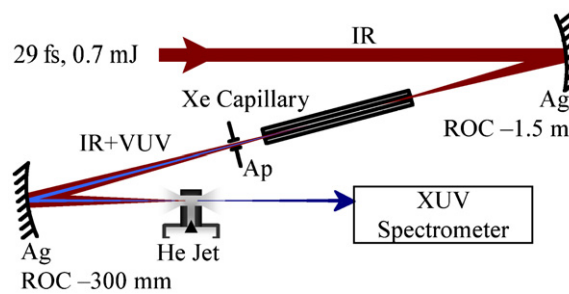


Figure 1. Experimental configuration. The IR laser generates VUV harmonics up to the 19th order in a Xe-filled capillary, which co-propagate and are used to manipulate XUV HHG in a pulsed He jet. The resulting VUV and XUV harmonics spectra are recorded using an XUV spectrometer. An aperture (Ap) is used to control the IR intensity in the interaction region.

The techniques of adaptive laser pulse shaping in the frequency [22–24] and spatial [25, 26] domain have also been used to spectrally control and increase the yield of HHG. In addition, quasi-phase matching has been extended from the visible and near infrared into the soft-x-ray regime [27]. In contrast to these methods, which rely on improved phase matching, Kim *et al* [28] have recently enhanced the single-atom HHG response by using an orthogonally polarized two-colour (fundamental and second harmonic) driving laser.

We report on the observation of HHG enhancement obtained by a superposition of a VUV pulse and a high-intensity IR pulse. The initial tunnel ionization step in the HHG process is assisted with a single VUV-photon ionization, which results in a large volume effect. Since the dependence of tunnel ionization on the IR intensity is highly nonlinear, IR-driven HHG is confined to a small volume around the peak of the IR beam. In contrast, VUV photoionization is a linear process and is therefore also effective in the low-intensity wings of the IR beam, which leads to HHG in a much larger volume. As a result, we predict enhanced HHG at moderate IR intensities [29].

Our prior publication [30] on VUV-assisted enhancement of HHG, consistent with our previous theoretical prediction, indicated the presence of phase-locked low-order harmonics, thereby indirectly suggesting the presence of an attosecond pulse train (APT). We support our initial experimental finding through a theoretical estimation of the influence of different low harmonic orders, from which an APT is synthesized, on the ionization step for HHG.

2. Experimental details

We present a first experimental demonstration of enhanced HHG in the XUV through a combination of strong low-order VUV harmonics and an IR laser field. A schematic of the experimental set-up is shown in figure 1.

The collinear configuration makes it easy to align and is particularly suitable for further applications. VUV harmonics are generated by loosely focusing a 29 fs (FWHM) IR pulse with a central wavelength of 785 nm and an energy of 0.7 mJ into the Xe-filled capillary with a spherical silver mirror (ROC = -1.5 m). The capillary has an inner diameter of 800 μm , a length of 50 mm and the focus is placed at the end of the capillary for maximum signal. Since the focus of the IR laser is five times smaller than the diameter of the capillary, we observe no guiding of the IR beam [31]. Xe is filled into the capillary from one end, at the laser entrance, at pressures between 0 and 25 mbar and is differentially pumped through the other end to

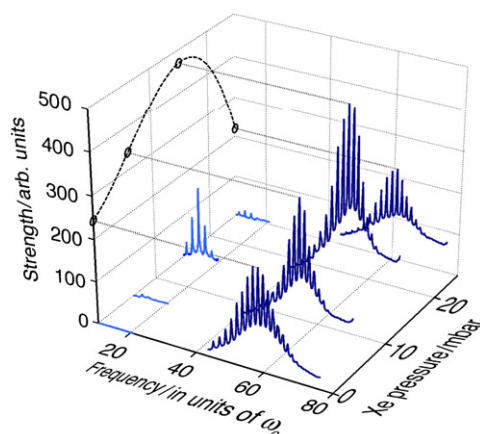


Figure 2. Enhancement of VUV-assisted HHG. The harmonic spectra of the VUV harmonics (left) and the XUV harmonics (right) are shown as a function of the Xe pressure, for a He jet backing pressure of 3 bar. The VUV harmonics strength diminishes for high pressures due to reabsorption. The harmonic plateau was experimentally not accessible due to the configuration of the measurement set-up.

ambient pressures below 10^{-3} mbar. The advantage of this configuration is that the capillary acts as a differential pumping stage, reducing the gas flow into the chamber compared to a pinhole of the same size. The drawback is that the resulting pressure gradient makes it difficult to know the precise gas distribution in the interaction region. We generate harmonics up to the 19th order, which translates to an IR peak intensity of 1×10^{14} W cm $^{-2}$ in the interaction region. The generated VUV and IR co-propagate through an adjustable aperture to a focusing mirror (silver, ROC = -300 mm, reflectivity $\sim 5\%$ at harmonic 15), before reaching the He target after 103 cm. The set-up is differentially pumped between the capillary exit and the He target in order to minimize VUV absorption during propagation. The adjustable aperture is placed at a distance of 62 cm after the capillary exit in order to adjust/reduce the IR energy and, after initial optimization, kept constant for each experimental run. The aperture only affects the IR beam due to its much larger divergence compared to the VUV beam. Simulating the focusing geometry, we have chosen a condition such that the focal sizes of the VUV and IR beams are similar. The focus is placed before the gas jet for maximum signal. We generate harmonics with the IR alone with a cut-off around order 69 in He, from which we estimate the IR peak intensity to 5×10^{14} W cm $^{-2}$ in the interaction region, corresponding to a focus size of $50 \mu\text{m}$ diameter. This cut-off does not change significantly with the Xe gas present (see figure 2). The He gas target consists of a pulsed, T-shaped tubular jet with an inner diameter of $260 \mu\text{m}$ and a length of 2 mm, where the laser passes along the tube length. A piezoelectric plunger synchronized with the laser fills the target from a gas reservoir with a backing pressure of up to 3 bar. The additional gas load increases the backing pressure in the vacuum chamber to almost 10^{-2} mbar. The generated VUV-assisted high harmonics propagate 1.7 m through differential pumping sections to an XUV spectrometer (McPherson) fibre-coupled to a CCD camera.

3. Results and discussion

Results of our measurements are shown in figure 2, where the spectral intensities measured for the input VUV (left) and generated XUV harmonics (right) are shown as a function of the Xe

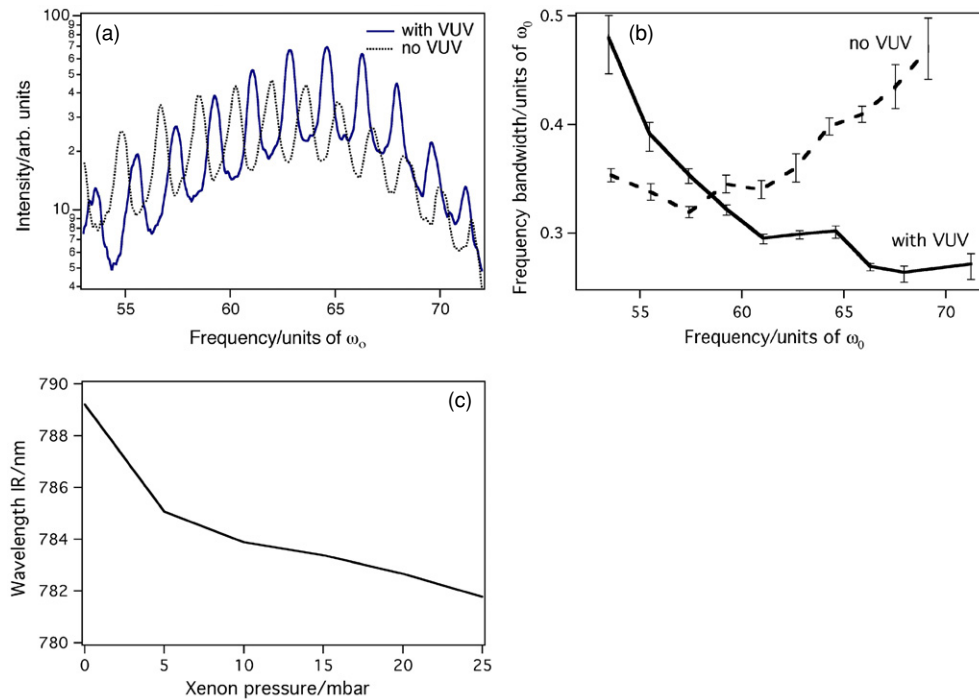


Figure 3. (a) XUV harmonic spectrum for a He jet backing pressure of 3 bar, with and without VUV assistance in the XUV HHG. (b) The spectral widths as a function of harmonic order. (c) Blue shift of the IR pulse after focusing in a gas cell filled with Xe at various pressures.

pressure within the capillary keeping all other parameters constant. The VUV harmonics were completely absorbed by He in the presence of the strong IR field and were measured using identical configuration, but with the He jet shortly switched off. To investigate whether He absorbs VUV harmonics, before entering the interaction region, we reduced the IR intensity by closing the aperture. We found that VUV harmonics with photon energy below the ionization threshold of He are no longer completely absorbed by the He gas.

The strengths of the VUV harmonics are observed to increase up to a Xe pressure of 15 mbar, followed by a decrease at higher pressures due to reabsorption in the Xe. The high harmonics generated within the He jet are observed to follow the VUV harmonic strength, illustrating that the VUV harmonics do increase the XUV yield. The simulations indeed predict a moderate enhancement of the cut-off harmonics, with the most dramatic (orders of magnitude) enhancement for the plateau harmonics. Our present set-up, unfortunately, did not allow us to observe the low-plateau harmonics, and therefore only the enhancement effect in the higher harmonics could be observed.

The generated XUV harmonics in figure 3(a) show a variation of the spectral width and a blue shift with increasing Xe pressure keeping all other parameters constant [32]. The spectral widths of individual harmonics within each HHG spectrum show a markedly different trend with and without VUV-assisted ionization, as shown in figure 3(b). Without the VUV harmonics, the higher orders exhibit a larger spectral bandwidth, whereas the VUV-assisted harmonics show a decreasing bandwidth with increasing order. The decrease in the harmonic bandwidth might be caused by a change in the IR chirp after propagation through Xe [22], but

warrants a theoretical investigation. Since we are reporting on novel observations, we find it convenient to include such a finding in order to stimulate further experimental and theoretical investigations on this aspect. We also expect the coherence properties of the XUV harmonics to be different compared to tunnel-ionization-based HHG. Blue shifting of XUV harmonics can be due to ionization by the VUV harmonics as well as blue shifting of the IR field. Due to the fact that the XUV harmonics blue shift and the spacing between consecutive harmonics continuously increase with increasing Xe pressure, but the VUV yield decreases again beyond 15 mbar of Xe, we can attribute the blue shift to the IR field propagating through increasingly ionized Xe.

We have measured an IR pulse with SPIDER after propagation through a gas cell filled with Xe. The pulse envelope, the energy and the divergence of the IR pulse were not significantly affected, but the centre of the spectrum was shifted by 7 nm after propagation through 25 mbar of Xe compared to the Xe-free case in close agreement with the observed blue shift of the XUV harmonics (figure 3(c)).

Our experimental demonstration that VUV harmonics can be used to enhance HHG leaves open the exact mechanism by which this comes about. Our previous theoretical studies have shown that phase-locked VUV harmonics (the 11th to 19th) which form an APT can be used to enhance HHG [33]. The large enhancement results from the change in the IR-intensity dependence of the harmonics caused by the APT's presence and timing relative to the IR field. First the different IR-intensity dependence of the generated harmonics results in a larger generation volume, which is very sensitive to the overlap of the VUV harmonics and the IR. A change in the beam sizes when the Xe pressure is varied cannot be ruled out and can have an effect on the generation efficiency of He. Second an APT would allow us to select the timing of the ionization of the electron into the continuum such that its ionization coincides with the release time to contribute to HHG. The enhancement is expected to be greatest under conditions that would otherwise yield low photon numbers, and enhancements of up to 2–4 orders of magnitude are predicted. At favourable delays, an APT-assisted HHG should result in a comb of clearly resolved harmonics of increasing width for increasing order. Significant enhancement is predicted in all cases, even at unfavourable delays where the ionization time fixed by the APT does not allow the returning electron wave packet to efficiently recombine with the parent ion.

Using all VUV light from the Xe capillary, and not just orders above 11, raises the question of how efficient the various harmonics are at generating harmonics in He. At a low IR intensity, harmonics below the 13th order cannot contribute to HHG, since they cannot ionize He directly or via a possibly resonantly enhanced single photon transition, which is commensurate with the 15th harmonic. However, at higher IR intensities this picture is strongly modified due to the distortion of the Coulomb potential by the strong field. To investigate this effect, we have calculated the relative efficiency of ionization with each of the harmonics from the 5th to the 13th order separately in the presence of a strong IR field of different intensities. To separate the VUV-driven ionization from tunnel ionization caused by the IR field we have solved an approximate time-dependent Schrödinger equation in the single active electron approximation [34, 35] for two fields (IR + VUV) that restricts the ionization to be driven just by the VUV field, but propagates the electron thereafter in the full atomic potential modified by the strong IR field. The harmonic fields are assumed to have a 5 fs FWHM Gaussian pulse shape. The ionization yield from each harmonic is normalized to the ionization yield of the 9th harmonic. Figure 4 shows that at a relatively low intensity the 13th harmonic ionizes about 10^{10} times more strongly than the 5th harmonic. However, by the time the peak intensity reaches $4 \times 10^{14} \text{ W cm}^{-2}$, which is near the intensity used in this experiment, the distribution flattens out considerably, and the 13th harmonic ionizes only about 100 times as much as the 5th. The

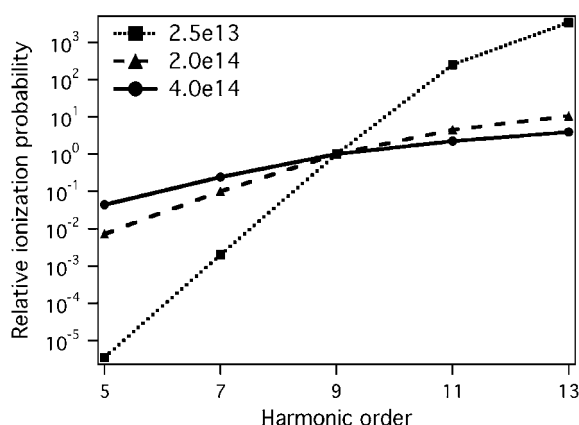


Figure 4. Relative He ionization probability as a function of harmonic order for different IR intensities, where the ionization yield of the 9th harmonic is normalized in each curve.

process of initiating HHG via ionization by low-order harmonics is complex, since ionization radially and temporally depends on the intensity of the IR pulse and therefore varies with low harmonic order. We conclude that filtering of the low-order harmonics and a direct measurement of an APT via, e.g. a RABITT measurement, are necessary to unequivocally prove the time dependence of VUV-assisted HHG in He.

We therefore expect that a future experiment will greatly benefit from an independent relative time control between the two colours (VUV + IR) in order to enhance the single-atom response together with favourable phase-matching conditions as predicted by our theory.

4. Conclusions

We have presented first the results of enhancement in harmonic yield due to VUV-assisted HHG in He. The initial tunnel ionization step in the HHG process is replaced with single VUV-photon ionization, which results in a large volume effect. It is predicted that ionization with APTs in the VUV regime could result in even higher enhancements by several orders of magnitude if the timing between the VUV and IR fields is chosen such that the single-atom and phase-matching effects both positively add to HHG.

Acknowledgments

We thank Mette B Gaarde and Kenneth J Schafer for the calculations on the ionization of He and many stimulating discussions. This work was supported by the Swiss National Science Foundation (QP-NCCR) and by ETH Zurich. We acknowledge the support of EU FP 6 program ‘Structuring the European Research Area’, Marie Curie Research Training Network XTRA (contract no FP6-505138).

References

- [1] McPherson A, Gibson G, Jara H, Johann U, Luk T S, McIntyre I, Boyer K and Rhodes C K 1987 *J. Opt. Soc. Am. B* **4** 595–601

- [2] Ferray M, L'Huillier A, Li X F, Lompré L A, Mainfray G and Manus C 1988 *J. Phys. B: At. Mol. Opt. Phys.* **21** L31–L35
- [3] Macklin J J, Kmetec J D and Gordon C L 1993 *Phys. Rev. Lett.* **70** 766
- [4] L'Huillier A and Balcou P 1993 *Phys. Rev. Lett.* **70** 774
- [5] Spielmann C, Burnett N H, Sartania S, Koppitsch R, Schnurer M, Kan C, Lenzner M, Wobrauschek P and Krausz F 1997 *Science* **278** 661
- [6] Seres J, Seres E, Verhoef A J, Tempea G, Strelci C, Wobrauschek P, Yakovlev V, Scrinzi A, Spielmann C and Krausz F 2005 *Nature* **433** 596
- [7] Krause J L, Schafer K J and Kullander K C 1992 *Phys. Rev. Lett.* **68** 3535
- [8] Corkum P B 1993 *Phys. Rev. Lett.* **71** 1994
- [9] Lewenstein M, Balcou P, Ivanov M Y, L'Huillier A and Corkum P B 1994 *Phys. Rev. A* **49** 2117
- [10] Schafer K J, Yang B, DiMauro L F and Kullander K C 1993 *Phys. Rev. Lett.* **70** 1599
- [11] Salières P, L'Huillier A and Lewenstein M 1995 *Phys. Rev. Lett.* **74** 3776
- [12] Roos L, Constant E, Mével E, Balcou P, Descamps D, Gaarde M B, Valette A, Haroutunian R and L'Huillier A 1999 *Phys. Rev. A* **60** 5010
- [13] Lompre L A, L'Huillier A, Ferray M, Monot P, Mainfray G and Manus C 1990 *J. Opt. Soc. Am. B* **7** 754
- [14] Kazamias S, Weihe F, Douillet D, Valentin C, Planchon T, Sebban S, Grillon G, Augé F, Hulin D and Balcou P 2002 *Eur. Phys. J. D* **21** 353
- [15] Takahashi E, Nabekawa Y, Otsuka T, Obara M and Midorikawa K 2002 *Phys. Rev. A* **66** 021802
- [16] Herrgott J-F, Kovacev M, Merdji H, Hubert C, Mairesse Y, Jean E, Breger P, Agostini P, Carré B and Salières P 2002 *Phys. Rev. A* **66** 021801
- [17] Takahashi E, Nabekawa Y and Midorikawa K 2004 *Appl. Phys. Lett.* **84** 4
- [18] Rundquist A, Durfee C G, Chang Z, Herne C, Backus S, Murnane M M and Kapteyn H C 1998 *Science* **280** 1412
- [19] Tamaki Y, Itatani J, Nagata Y, Obara M and Midorikawa K 1999 *Phys. Rev. Lett.* **82** 1422
- [20] Constant E, Garzella D, Breger P, Mével E, Dorrier C, Blanc C L, Salin F and Agostini P 1999 *Phys. Rev. Lett.* **82** 1668
- [21] Kazamias S, Douillet D, Weihe F, Valentin C, Rousse A, Sebban S, Grillon G F A, Hulin D and Balcou P 2003 *Phys. Rev. Lett.* **90** 193901
- [22] Bartels R, Backus S, Zeek E, Misoguti L, Vdovin G, Christov I P, Murnane M M and Kapteyn H C 2000 *Nature* **406** 164
- [23] Reitze D H, Weiner A M and Leaird D E 1992 *Appl. Phys. Lett.* **61** 1260
- [24] Pfeifer T, Walter D, Winterfeldt C, Spielmann C and Gerber G 2004 *Appl. Phys. B* **80** 277
- [25] Villoresi P, Bonora S, Pascolini M, Poletto L, Tondello G, Vozzi C, Nisoli M, Sansone G, Stagira S and Silvestri S D 2004 *Opt. Lett.* **29** 207
- [26] Pfeifer T, Kemmer R, Spitzenpfeil R, Walter D, Winterfeldt C, Gerber G and Spielmann C 2005 *Opt. Lett.* **30** 1497
- [27] Gibson E A *et al* 2003 *Science* **302** 95
- [28] Kim I J, Kim C M, Kim H T, Lee G H, Lee Y S, Park J Y, Cho D J and Nam C H 2005 *Phys. Rev. Lett.* **94** 243901
- [29] Gaarde M B, Schafer K J, Heinrich A, Biegert J and Keller U 2005 *Phys. Rev. A* **72** 013411
- [30] Biegert J, Heinrich A, Hauri C P, Kornelis W, Schlup P, Ansonbe M, Schafer K J, Gaarde M B and Keller U 2005 *Laser Phys.* **15** 899–902
- [31] Nisoli M, Silvestri S D and Svelto O 1996 *Appl. Phys. Lett.* **68** 2793
- [32] Altucci C *et al* 2000 *Phys. Rev. A* **61** 021801
- [33] Schafer K J, Gaarde M B, Heinrich A, Biegert J and Keller U 2004 *Phys. Rev. Lett.* **92** 023003
- [34] Kullander K C, Schafer K J and Krause J L 1992 *Atoms in Intense Laser Fields* (San Diego: Academic)
- [35] Schafer K J and Kullander K C 1997 *Phys. Rev. Lett.* **78** 638–71